

Observation of D^0 - \bar{D}^0 Mixing using the CDF II Detector

T. Aaltonen,²¹ S. Amerio^{kk, 39} D. Amidei,³¹ A. Anastassov^{w, 15} A. Annovi,¹⁷ J. Antos,¹² G. Apollinari,¹⁵ J.A. Appel,¹⁵ T. Arisawa,⁵² A. Artikov,¹³ J. Asaadi,⁴⁷ W. Ashmanskas,¹⁵ B. Auerbach,² A. Aurisano,⁴⁷ F. Azfar,³⁸ W. Badgett,¹⁵ T. Bae,²⁵ A. Barbaro-Galtieri,²⁶ V.E. Barnes,⁴³ B.A. Barnett,²³ J. Guimaraes da Costa,²⁰ P. Barria^{mm, 41} P. Bartos,¹² M. Bauc^{kk, 39} F. Bedeschi,⁴¹ S. Behari,¹⁵ G. Bellettini^{ll, 41} J. Bellinger,⁵⁴ D. Benjamin,¹⁴ A. Beretvas,¹⁵ A. Bhatti,⁴⁵ K.R. Bland,⁵ B. Blumenfeld,²³ A. Bocci,¹⁴ A. Bodek,⁴⁴ D. Bortoletto,⁴³ J. Boudreau,⁴² A. Boveia,¹¹ L. Brigliadori^{jj, 6} C. Bromberg,³² E. Brucken,²¹ J. Budagov,¹³ H.S. Budd,⁴⁴ K. Burkett,¹⁵ G. Busetto^{kk, 39} P. Bussey,¹⁹ P. Butti^{ll, 41} A. Buzatu,¹⁹ A. Calamba,¹⁰ S. Camarda,⁴ M. Campanelli,²⁸ F. Canelli^{dd, 11} B. Carls,²² D. Carlsmith,⁵⁴ R. Carosi,⁴¹ S. Carrillo^{l, 16} B. Casal^{j, 9} M. Casarsa,⁴⁸ A. Castro^{jj, 6} P. Catastini,²⁰ D. Cauz^{rrss, 48} V. Cavaliere,²² M. Cavalli-Sforza,⁴ A. Cerri^{e, 26} L. Cerrito^{r, 28} Y.C. Chen,¹ M. Chertok,⁷ G. Chiarelli,⁴¹ G. Chlachidze,¹⁵ K. Cho,²⁵ D. Chokheli,¹³ A. Clark,¹⁸ C. Clarke,⁵³ M.E. Convery,¹⁵ J. Conway,⁷ M. Corbo^{z, 15} M. Cordelli,¹⁷ C.A. Cox,⁷ D.J. Cox,⁷ M. Cremonesi,⁴¹ D. Cruz,⁴⁷ J. Cuevas^{y, 9} R. Culbertson,¹⁵ N. d'Ascenzo^{v, 15} M. Datta^{gg, 15} P. de Barbaro,⁴⁴ L. Demortier,⁴⁵ M. Deninno,⁶ M. D'Errico^{kk, 39} F. Devoto,²¹ A. Di Canto^{ll, 41} B. Di Ruzza^{p, 15} J.R. Dittmann,⁵ S. Donati^{ll, 41} M. D'Onofrio,²⁷ M. Dorigo^{tt, 48} A. Driutti^{rrss, 48} K. Ebina,⁵² R. Edgar,³¹ A. Elagin,⁴⁷ R. Erbacher,⁷ S. Errede,²² B. Esham,²² S. Farrington,³⁸ J.P. Fernández Ramos,²⁹ R. Field,¹⁶ G. Flanagan^{t, 15} R. Forrest,⁷ M. Franklin,²⁰ J.C. Freeman,¹⁵ H. Frisch,¹¹ Y. Funakoshi,⁵² C. Galloni^{ll, 41} A.F. Garfinkel,⁴³ P. Garosi^{mm, 41} H. Gerberich,²² E. Gerchtein,¹⁵ S. Giagu,⁴⁶ V. Giakoumopoulou,³ K. Gibson,⁴² C.M. Ginsburg,¹⁵ N. Giokaris,³ P. Giomini,¹⁷ G. Giurgiu,²³ V. Glagolev,¹³ D. Glenzinski,¹⁵ M. Gold,³⁴ D. Goldin,⁴⁷ A. Golossanov,¹⁵ G. Gomez,⁹ G. Gomez-Ceballos,³⁰ M. Goncharov,³⁰ O. González López,²⁹ I. Gorelov,³⁴ A.T. Goshaw,¹⁴ K. Goulianos,⁴⁵ E. Gramellini,⁶ S. Grinstein,⁴ C. Grosso-Pilcher,¹¹ R.C. Group,^{51, 15} S.R. Hahn,¹⁵ J.Y. Han,⁴⁴ F. Happacher,¹⁷ K. Hara,⁴⁹ M. Hare,⁵⁰ R.F. Harr,⁵³ T. Harrington-Taber^{m, 15} K. Hatakeyama,⁵ C. Hays,³⁸ J. Heinrich,⁴⁰ M. Herndon,⁵⁴ A. Hocker,¹⁵ Z. Hong,⁴⁷ W. Hopkins^{f, 15} S. Hou,¹ R.E. Hughes,³⁵ U. Husemann,⁵⁵ M. Hussein^{bb, 32} J. Huston,³² G. Introzzi^{oop, 41} M. Iori^{qq, 46} A. Ivanov^{o, 7} E. James,¹⁵ D. Jang,¹⁰ B. Jayatilaka,¹⁵ E.J. Jeon,²⁵ S. Jindariani,¹⁵ M. Jones,⁴³ K.K. Joo,²⁵ S.Y. Jun,¹⁰ T.R. Junk,¹⁵ M. Kambeitz,²⁴ T. Kamon,^{25, 47} P.E. Karchin,⁵³ A. Kasmi,⁵ Y. Kato^{n, 37} W. Ketchum^{hh, 11} J. Keung,⁴⁰ B. Kilminster^{dd, 15} D.H. Kim,²⁵ H.S. Kim,²⁵ J.E. Kim,²⁵ M.J. Kim,¹⁷ S.H. Kim,⁴⁹ S.B. Kim,²⁵ Y.J. Kim,²⁵ Y.K. Kim,¹¹ N. Kimura,⁵² M. Kirby,¹⁵ K. Knoepfel,¹⁵ K. Kondo,^{52, *} D.J. Kong,²⁵ J. Konigsberg,¹⁶ A.V. Kotwal,¹⁴ M. Kreps,²⁴ J. Kroll,⁴⁰ M. Kruse,¹⁴ T. Kuhr,²⁴ N. Kulkarni,⁵³ M. Kurata,⁴⁹ A.T. Laasanen,⁴³ S. Lammel,¹⁵ M. Lancaster,²⁸ K. Lannon^{x, 35} G. Latino^{mm, 41} H.S. Lee,²⁵ J.S. Lee,²⁵ S. Leo,⁴¹ S. Leone,⁴¹ J.D. Lewis,¹⁵ A. Limosani^{s, 14} E. Lipeles,⁴⁰ A. Lister^{a, 18} H. Liu,⁵¹ Q. Liu,⁴³ T. Liu,¹⁵ S. Lockwitz,⁵⁵ A. Loginov,⁵⁵ D. Lucchesi^{kk, 39} A. Lucà,¹⁷ J. Lueck,²⁴ P. Lujan,²⁶ P. Lukens,¹⁵ G. Lungu,⁴⁵ J. Lys,²⁶ R. Lysak^{d, 12} R. Madrak,¹⁵ P. Maestro^{mm, 41} S. Malik,⁴⁵ G. Manca^{b, 27} A. Manousakis-Katsikakis,³ L. Marchese^{ii, 6} F. Margaroli,⁴⁶ P. Marino^{nn, 41} M. Martínez,⁴ K. Matera,²² M.E. Mattson,⁵³ A. Mazzacane,¹⁵ P. Mazzanti,⁶ R. McNulty^{i, 27} A. Mehta,²⁷ P. Mehtala,²¹ C. Mesropian,⁴⁵ T. Miao,¹⁵ D. Mietlicki,³¹ A. Mitra,¹ H. Miyake,⁴⁹ S. Moed,¹⁵ N. Moggi,⁶ C.S. Moon^{z, 15} R. Moore^{eeff, 15} M.J. Morello^{nn, 41} A. Mukherjee,¹⁵ Th. Muller,²⁴ P. Murat,¹⁵ M. Mussini^{jj, 6} J. Nachtman^{m, 15} Y. Nagai,⁴⁹ J. Naganoma,⁵² I. Nakano,³⁶ A. Napier,⁵⁰ J. Nett,⁴⁷ C. Neu,⁵¹ T. Nigmanov,⁴² L. Nodulman,² S.Y. Noh,²⁵ O. Norniella,²² L. Oakes,³⁸ S.H. Oh,¹⁴ Y.D. Oh,²⁵ I. Oksuzian,⁵¹ T. Okusawa,³⁷ R. Orava,²¹ L. Ortolan,⁴ C. Pagliarone,⁴⁸ E. Palencia^{e, 9} P. Palni,³⁴ V. Papadimitriou,¹⁵ W. Parker,⁵⁴ G. Pauletta^{rrss, 48} M. Paulini,¹⁰ C. Paus,³⁰ T.J. Phillips,¹⁴ G. Piacentino,⁴¹ E. Pianori,⁴⁰ J. Pilot,⁷ K. Pitts,²² C. Plager,⁸ L. Pondrom,⁵⁴ S. Poprocki^{f, 15} K. Potamianos,²⁶ A. Pranko,²⁶ F. Prokoshin^{aa, 13} F. Ptohos^{g, 17} G. Punzi^{ll, 41} N. Ranjan,⁴³ I. Redondo Fernández,²⁹ P. Renton,³⁸ M. Rescigno,⁴⁶ F. Rimondi,^{6, *} L. Ristori,^{41, 15} A. Robson,¹⁹ T. Rodriguez,⁴⁰ S. Rolli^{h, 50} M. Ronzani^{ll, 41} R. Roser,¹⁵ J.L. Rosner,¹¹ F. Ruffini^{mm, 41} A. Ruiz,⁹ J. Russ,¹⁰ V. Rusu,¹⁵ W.K. Sakumoto,⁴⁴ Y. Sakurai,⁵² L. Santi^{rrss, 48} K. Sato,⁴⁹ V. Saveliev^{v, 15} A. Savoy-Navarro^{z, 15} P. Schlabach,¹⁵ E.E. Schmidt,¹⁵ T. Schwarz,³¹ L. Scodellaro,⁹ F. Scuri,⁴¹ S. Seidel,³⁴ Y. Seiya,³⁷ A. Semenov,¹³ F. Sforza^{ll, 41} S.Z. Shalhout,⁷ T. Shears,²⁷ P.F. Shepard,⁴² M. Shimojima^{u, 49} M. Shochet,¹¹ A. Simonenko,¹³ K. Sliwa,⁵⁰ J.R. Smith,⁷ F.D. Snider,¹⁵ H. Song,⁴² V. Sorin,⁴ R. St. Denis,¹⁹ M. Stancari,¹⁵ D. Stentz^{w, 15} J. Strologas,³⁴ Y. Sudo,⁴⁹ A. Sukhanov,¹⁵ I. Suslov,¹³ K. Takemasa,⁴⁹ Y. Takeuchi,⁴⁹ J. Tang,¹¹ M. Tecchio,³¹ I. Shreyber-Tecker,³³ P.K. Teng,¹ J. Thom^{f, 15} E. Thomson,⁴⁰ V. Thukral,⁴⁷ D. Toback,⁴⁷ S. Tokar,¹² K. Tollefson,³² T. Tomura,⁴⁹ D. Tonelli^{e, 15} S. Torre,¹⁷ D. Torretta,¹⁵ P. Totaro,³⁹ M. Trovato^{nn, 41} F. Ukegawa,⁴⁹ S. Uozumi,²⁵ F. Vázquez^{l, 16} G. Velev,¹⁵ C. Vellidis,¹⁵ C. Vernieri^{nn, 41} M. Vidal,⁴³ R. Vilar,⁹ J. Vizán^{cc, 9} M. Vogel,³⁴ G. Volpi,¹⁷ P. Wagner,⁴⁰ R. Wallny^{j, 15} S.M. Wang,¹ D. Waters,²⁸

W.C. Wester III,¹⁵ D. Whiteson^{c, 40} A.B. Wicklund,² S. Wilbur,⁷ H.H. Williams,⁴⁰ J.S. Wilson,³¹ P. Wilson,¹⁵
 B.L. Winer,³⁵ P. Wittich^{f, 15} S. Wolbers,¹⁵ H. Wolfe,³⁵ T. Wright,³¹ X. Wu,¹⁸ Z. Wu,⁵ K. Yamamoto,³⁷
 D. Yamato,³⁷ T. Yang,¹⁵ U.K. Yang,²⁵ Y.C. Yang,²⁵ W.-M. Yao,²⁶ G.P. Yeh,¹⁵ K. Yi^{m, 15} J. Yoh,¹⁵
 K. Yorita,⁵² T. Yoshida^{k, 37} G.B. Yu,¹⁴ I. Yu,²⁵ A.M. Zanetti,⁴⁸ Y. Zeng,¹⁴ C. Zhou,¹⁴ and S. Zucchelli^{jj6}
 (CDF Collaboration)[†]

¹*Institute of Physics, Academia Sinica, Taipei, Taiwan 11529, Republic of China*

²*Argonne National Laboratory, Argonne, Illinois 60439, USA*

³*University of Athens, 157 71 Athens, Greece*

⁴*Institut de Fisica d'Altes Energies, ICREA, Universitat Autònoma de Barcelona, E-08193, Bellaterra (Barcelona), Spain*

⁵*Baylor University, Waco, Texas 76798, USA*

⁶*Istituto Nazionale di Fisica Nucleare Bologna, ^{jj}University of Bologna, I-40127 Bologna, Italy*

⁷*University of California, Davis, Davis, California 95616, USA*

⁸*University of California, Los Angeles, Los Angeles, California 90024, USA*

⁹*Instituto de Fisica de Cantabria, CSIC-University of Cantabria, 39005 Santander, Spain*

¹⁰*Carnegie Mellon University, Pittsburgh, Pennsylvania 15213, USA*

¹¹*Enrico Fermi Institute, University of Chicago, Chicago, Illinois 60637, USA*

¹²*Comenius University, 842 48 Bratislava, Slovakia; Institute of Experimental Physics, 040 01 Kosice, Slovakia*

¹³*Joint Institute for Nuclear Research, RU-141980 Dubna, Russia*

¹⁴*Duke University, Durham, North Carolina 27708, USA*

¹⁵*Fermi National Accelerator Laboratory, Batavia, Illinois 60510, USA*

¹⁶*University of Florida, Gainesville, Florida 32611, USA*

¹⁷*Laboratori Nazionali di Frascati, Istituto Nazionale di Fisica Nucleare, I-00044 Frascati, Italy*

¹⁸*University of Geneva, CH-1211 Geneva 4, Switzerland*

¹⁹*Glasgow University, Glasgow G12 8QQ, United Kingdom*

²⁰*Harvard University, Cambridge, Massachusetts 02138, USA*

²¹*Division of High Energy Physics, Department of Physics, University of Helsinki, FIN-00014, Helsinki, Finland; Helsinki Institute of Physics, FIN-00014, Helsinki, Finland*

²²*University of Illinois, Urbana, Illinois 61801, USA*

²³*The Johns Hopkins University, Baltimore, Maryland 21218, USA*

²⁴*Institut für Experimentelle Kernphysik, Karlsruhe Institute of Technology, D-76131 Karlsruhe, Germany*

²⁵*Center for High Energy Physics: Kyungpook National University, Daegu 702-701, Korea; Seoul National University, Seoul 151-742, Korea; Sungkyunkwan University, Suwon 440-746, Korea; Korea Institute of Science and Technology Information, Daejeon 305-806, Korea; Chonnam National University, Gwangju 500-757, Korea; Chonbuk National University, Jeonju 561-756, Korea; Ewha Womans University, Seoul, 120-750, Korea*

²⁶*Ernest Orlando Lawrence Berkeley National Laboratory, Berkeley, California 94720, USA*

²⁷*University of Liverpool, Liverpool L69 7ZE, United Kingdom*

²⁸*University College London, London WC1E 6BT, United Kingdom*

²⁹*Centro de Investigaciones Energeticas Medioambientales y Tecnologicas, E-28040 Madrid, Spain*

³⁰*Massachusetts Institute of Technology, Cambridge, Massachusetts 02139, USA*

³¹*University of Michigan, Ann Arbor, Michigan 48109, USA*

³²*Michigan State University, East Lansing, Michigan 48824, USA*

³³*Institution for Theoretical and Experimental Physics, ITEP, Moscow 117259, Russia*

³⁴*University of New Mexico, Albuquerque, New Mexico 87131, USA*

³⁵*The Ohio State University, Columbus, Ohio 43210, USA*

³⁶*Okayama University, Okayama 700-8530, Japan*

³⁷*Osaka City University, Osaka 558-8585, Japan*

³⁸*University of Oxford, Oxford OX1 3RH, United Kingdom*

³⁹*Istituto Nazionale di Fisica Nucleare, Sezione di Padova, ^{kk}University of Padova, I-35131 Padova, Italy*

⁴⁰*University of Pennsylvania, Philadelphia, Pennsylvania 19104, USA*

⁴¹*Istituto Nazionale di Fisica Nucleare Pisa, ^{ll}University of Pisa, ^{mm}University of Siena, ⁿⁿScuola Normale Superiore, I-56127 Pisa, Italy, ^{oo}INFN Pavia, I-27100 Pavia, Italy, ^{pp}University of Pavia, I-27100 Pavia, Italy*

⁴²*University of Pittsburgh, Pittsburgh, Pennsylvania 15260, USA*

⁴³*Purdue University, West Lafayette, Indiana 47907, USA*

⁴⁴*University of Rochester, Rochester, New York 14627, USA*

⁴⁵*The Rockefeller University, New York, New York 10065, USA*

⁴⁶*Istituto Nazionale di Fisica Nucleare, Sezione di Roma 1, ^{qq}Sapienza Università di Roma, I-00185 Roma, Italy*

⁴⁷*Mitchell Institute for Fundamental Physics and Astronomy,
Texas A&M University, College Station, Texas 77843, USA*

⁴⁸*Istituto Nazionale di Fisica Nucleare Trieste, ^{rr} Gruppo Collegato di Udine,*

^{ss}*University of Udine, I-33100 Udine, Italy, ^{tt} University of Trieste, I-34127 Trieste, Italy*

⁴⁹*University of Tsukuba, Tsukuba, Ibaraki 305, Japan*

⁵⁰*Tufts University, Medford, Massachusetts 02155, USA*

⁵¹*University of Virginia, Charlottesville, Virginia 22906, USA*

⁵²*Waseda University, Tokyo 169, Japan*

⁵³*Wayne State University, Detroit, Michigan 48201, USA*

⁵⁴*University of Wisconsin, Madison, Wisconsin 53706, USA*

⁵⁵*Yale University, New Haven, Connecticut 06520, USA*

(Dated: September 16, 2013)

We measure the time dependence of the ratio of decay rates for $D^0 \rightarrow K^+\pi^-$ to the Cabibbo-favored decay $D^0 \rightarrow K^-\pi^+$. The charge conjugate decays are included. A signal of 3.3×10^4 $D^{*+} \rightarrow \pi^+ D^0$, $D^0 \rightarrow K^+\pi^-$ decays is obtained with D^0 proper decay times between 0.75 and 10 mean D^0 lifetimes. The data were recorded with the CDF II detector at the Fermilab Tevatron and correspond to an integrated luminosity of 9.6 fb^{-1} for $p\bar{p}$ collisions at $\sqrt{s} = 1.96 \text{ TeV}$. Assuming CP conservation, we search for D^0 - \bar{D}^0 mixing and measure the mixing parameters to be $R_D = (3.51 \pm 0.35) \times 10^{-3}$, $y' = (4.3 \pm 4.3) \times 10^{-3}$, and $x'^2 = (0.08 \pm 0.18) \times 10^{-3}$. We report Bayesian probability intervals in the x'^2 - y' plane and find that the significance of excluding the no-mixing hypothesis is equivalent to 6.1 Gaussian standard deviations, providing the second observation of D^0 - \bar{D}^0 mixing from a single experiment.

PACS numbers: 12.15.Ff, 13.20.Fc, 13.25.Ft, 14.40.Lb

Keywords: charm, mixing

A neutral meson that is a superposition of weakly decaying mass eigenstates can spontaneously change into its antiparticle. This process is referred to as mixing and is well established for K^0 , B^0 , and B_s^0 mesons [1]. The mixing of these mesons is understood within the framework of the standard model with the Cabibbo-Kobayashi-Maskawa quark-mixing matrix. Substantial evidence exists for D^0 - \bar{D}^0 mixing [2–6], and the process was recently observed in the $K\pi$ channel by the LHCb experiment [7]. In the standard model, D^0 - \bar{D}^0 mixing is a weak-interaction process that occurs primarily through long-range virtual intermediate states that consist of common decay channels for particle and antiparticle, such as $\pi^+\pi^-$. The prediction of the mixing rate has significant uncertainty because it requires a strong-interaction model. A direct calculation from quantum chromodynamics is not currently possible [8, 9]. Mixing could also result from exotic particles that appear as virtual states in a short-range box diagram. Such a process could provide indirect evidence for physics beyond the standard model [10, 11]. It is of great interest to verify independently the observation of D^0 - \bar{D}^0 mixing in a single experiment and to improve the measurement of the mixing parameters. We report a measurement using the decay $D^0 \rightarrow K^+\pi^-$ and its charge conjugate.

The decay $D^0 \rightarrow K^+\pi^-$ can arise from mixing of a D^0 state to a \bar{D}^0 state, followed by a Cabibbo-favored (CF) decay, or from a doubly Cabibbo-suppressed (DCS) decay of a D^0 . (In this Letter, reference to a specific decay chain implicitly includes the charge-conjugate decay.) The mixing measurement is based on the ratio R of $D^0 \rightarrow K^+\pi^-$ to $D^0 \rightarrow K^-\pi^+$ decay rates. This ratio

can be approximated [12, 13] as a quadratic function of t/τ , where t is the proper decay time and τ is the mean D^0 lifetime:

$$R(t/\tau) = R_D + \sqrt{R_D} y' (t/\tau) + \frac{x'^2 + y'^2}{4} (t/\tau)^2. \quad (1)$$

This form is valid under the assumption of CP conservation and small values for the parameters $x = \Delta m/\Gamma$ and $y = \Delta\Gamma/2\Gamma$, where Δm is the mass difference between the mass eigenstates, $\Delta\Gamma$ is the decay-width difference, and Γ is the mean decay width of the eigenstates. The parameter R_D is the squared modulus of the ratio of DCS to CF amplitudes. The parameters x' and y' are linear combinations of x and y according to the relations

$$x' = x \cos \delta + y \sin \delta \quad \text{and} \quad y' = -x \sin \delta + y \cos \delta,$$

where δ is the strong-interaction phase difference between the DCS and CF amplitudes. In the absence of mixing, $x' = y' = 0$ and $R(t/\tau) = R_D$.

The measurement uses the full data set collected by the CDF II detector at the Fermilab Tevatron collider, from February 2002 to September 2011, corresponding to an integrated luminosity of 9.6 fb^{-1} for $p\bar{p}$ collisions at $\sqrt{s} = 1.96 \text{ TeV}$. We previously reported evidence for D^0 - \bar{D}^0 mixing [5] based on a subset of the data corresponding to an integrated luminosity of 1.5 fb^{-1} . The multipurpose CDF II detector [14] is a magnetic spectrometer surrounded by a calorimeter and a muon detector. The detector components pertinent to this analysis are the silicon microstrip vertex detector, the multi-wire drift chamber, and the 1.4 T magnet, which together measure the trajectories and momenta of charged particles. The

drift chamber measures ionization energy loss for charged particles, which is used for particle identification. Events are selected in real time with a trigger system developed for a broad class of heavy-flavor decays. The trigger [15] selects events with a pair of oppositely charged particles originating from a decay point separated by at least 200 μm from the beamline in the transverse plane.

We identify the CF decay $D^0 \rightarrow K^-\pi^+$ through the right-sign (RS) decay chain $D^{*+} \rightarrow \pi^+D^0$, $D^0 \rightarrow K^-\pi^+$. The decay $D^0 \rightarrow K^+\pi^-$ is identified through the wrong-sign (WS) decay chain $D^{*+} \rightarrow \pi^+D^0$, $D^0 \rightarrow K^+\pi^-$. The relative charges of the pions determine whether the decay chain is RS (same charge) or WS (opposite charge). The RS and WS D^* decays have the same kinematic distributions, and may differ only in decay time distributions. To reduce systematic uncertainties, we use the same selection criteria (cuts) for both the RS and WS decay modes. Analysis cuts were optimized before the WS candidates were revealed, and were chosen to maximize the expected WS signal significance.

The D^0 candidate reconstruction starts with a pair of tracks from oppositely-charged particles that satisfy the trigger requirements. The tracks are considered with both $K^-\pi^+$ and π^-K^+ interpretations. A third track, required to have transverse momentum in the range $[0.4, 2.0]$ GeV/c (see [16]), is used to form a D^* candidate when considered as a pion and combined with the D^0 candidate.

We use a method primarily based on D^0 decay kinematics to reduce the background to the WS signal from RS decays where the D^0 decay tracks are misidentified because the kaon and pion assignments are mistakenly interchanged. As determined from data for RS D^{*+} s, 96% of D^0 decays with correct mass assignments are reconstructed with invariant masses within 20 MeV/c^2 of the D^0 mass. The invariant mass distribution for misidentified D^0 decays is much broader, and has only 23% of the events within the same mass range. We remove WS candidates that have a RS mass within that range. To further reject D^* candidates with misidentified decay tracks, we impose a cut based on particle identification, described in Ref. [15], that is used to choose between $K^-\pi^+$ and π^-K^+ assignments for the D^0 decay tracks.

We use a series of cuts based on the decay topology of signal events in which the D^* is produced at the collision point and the D^0 travels a measurable distance before it decays. The topological cuts reduce background from combinations involving one or more tracks that do not originate from the D^* decay chain of interest. We require the significance of the transverse decay length to satisfy $L_{xy}/\sigma_{xy} > 4$, where L_{xy} is the distance between the collision point (measured on an event-by-event basis) and the reconstructed D^0 decay point in the plane transverse to the beamline, and σ_{xy} is the uncertainty on L_{xy} . The transverse impact parameter d_0 is the distance of closest approach in the transverse plane between a track

(or reconstructed particle) and the collision point. The D^* -decay pion must have $d_0 < 600 \mu\text{m}$, and it must also have a distance of closest approach to the collision point less than 1.5 cm along the beamline. To reduce the contribution of nonprompt D^* 's produced in beauty-particle decays, we require $d_0 < 60 \mu\text{m}$ for the inferred track of the D^0 candidate. The remaining contribution of nonprompt D^* mesons is taken into account in the analysis of the time dependence of the WS/RS ratio, as discussed later.

The ratio t/τ is determined for each D^0 candidate by $t/\tau = M_{D^0}L_{xy}/(p_T\tau)$, where $M_{D^0} = 1.8648 \text{ GeV}/c^2$ and $\tau = 410.1 \text{ fs}$ are the world-average values for the D^0 mass and lifetime, respectively [1]. To study $R(t/\tau)$, we divide the data into 20 bins of t/τ ranging from 0.75 to 10.0, choosing bins of increasing size from 0.25 to 2.0 to reduce statistical uncertainty per bin at larger times. The bin sizes are larger than the typical t/τ resolution of 0.16.

The RS and WS candidates in each t/τ bin are further divided into 60 bins of mass difference $\Delta M \equiv M_{K^+\pi^-\pi^+} - M_{K^+\pi^-} - M_{\pi^+}$ for WS candidates, and analogously for RS candidates. For each of the 1200 WS and 1200 RS ΔM bins, the D^0 signal yield is determined from a fit to the corresponding binned distribution of $M_{K\pi}$. In the fit, the signal shape is modeled by a double-Gaussian form with a low-mass tail, and the combinatorial background is modeled by an exponential. For the WS $M_{K\pi}$ fit, a Gaussian term models the RS background, with mean and width determined from the data. The D^* signal yield for each time bin is determined from a χ^2 fit of the D^0 signal yield versus ΔM . The signal shape is modeled by a double Gaussian and an asymmetric tail. The background shape is modeled by the product of a power law and an exponential function. The WS signal shape parameters for both the $M_{K\pi}$ and ΔM distributions are fixed to the RS parameters. For each $M_{K\pi}$ and ΔM distribution, the parameters for the background shape are allowed to float. The amplitudes of the signal and background are determined independently for all $M_{K\pi}$ and ΔM fits. The RS distributions have similar amounts of background as the WS distributions, but the RS signal is about 230 times larger. A detailed description of the functional forms for the signal and background shapes is presented in Ref. [16]. The $M_{K\pi}$ distributions from a subset of the data, which are characteristic of the full data set, are reported in [5, 15]. The 2400 $M_{K\pi}$ histograms are well fit by the functional form used; the distribution of χ^2/dof has a mean of 1.2 and a standard deviation of 0.4. The time-integrated WS ΔM distribution is shown in Fig. 1. The time-integrated signal yields are $(3.27 \pm 0.04) \times 10^4$ (WS) and $(7.604 \pm 0.005) \times 10^6$ (RS).

The measured ratio R_m of WS to RS signal for each of the 20 t/τ bins is shown in Fig. 2. The data point for each bin is located at the mean value of t/τ for the RS signal in that bin. Each error bar is determined from the fit

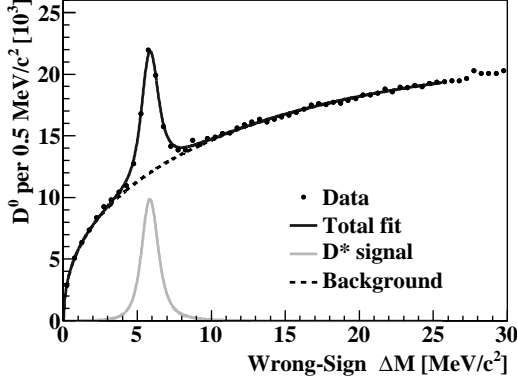


FIG. 1. Time-integrated distribution for wrong-sign $D^0 \rightarrow K^+\pi^-$ signal yield as a function of ΔM . The signal yield for each bin of ΔM is determined from a fit to the corresponding $M_{K\pi}$ distribution. The result of a χ^2 fit to the ΔM distribution is shown.

uncertainties of the WS and RS signal yields. The large uncertainty in the smallest t/τ bin is due to the small event yield caused by the trigger turn-on. After the trigger turn-on, the uncertainties increase with t/τ because of the exponential fall-off in the number of decays.

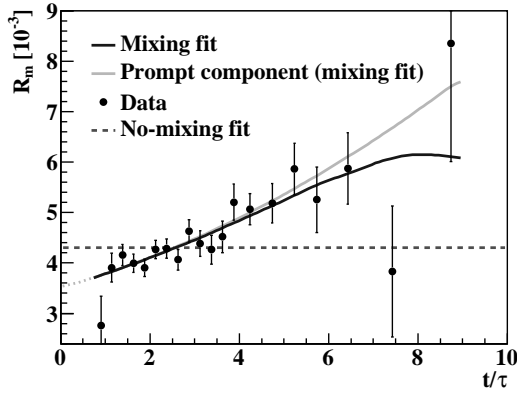


FIG. 2. Measured ratio R_m of wrong-sign to right-sign D^* decays as a function of normalized proper decay time. The results of a least-squares fit are shown for R_m^{pred} (mixing fit) and the prompt component R . A fit assuming no mixing is clearly incompatible with the data.

We assume that the WS/RS ratio of decay rates $R(t/\tau)$, given by Eq. (1), is the same for D^0 's produced in beauty-particle decays as for promptly-produced D^0 's, but with decay time measured from the beauty-particle decay point. The predicted value of R_m for a given t/τ bin can be expressed in terms of contributions from prompt and nonprompt production according to

$$R_m^{pred} = R(t/\tau) [1 - f_B(t/\tau)] + R_B(t/\tau) f_B(t/\tau), \quad (2)$$

where $f_B(t/\tau)$ is the fraction of nonprompt RS D^* decays and $R_B(t/\tau)$ is the WS/RS ratio of nonprompt D^* decays. For nonprompt decays, the measured decay time is due to the combination of the decay times for the beauty-particle parent and its D^0 daughter. The function $f_B(t/\tau)$ is determined from data, and $R_B(t/\tau)$ is determined from a full detector simulation.

The function $f_B(t)$ is determined from the d_0 distribution of D^0 's from RS D^* decays, as illustrated in Fig. 3. For each bin of t/τ , the d_0 distribution is obtained by selecting RS events with $4 < \Delta M < 8 \text{ MeV}/c^2$ and $1.848 < M_{K\pi} < 1.880 \text{ GeV}/c^2$ ($\pm 2\sigma$) and subtracting background determined from the $M_{K\pi}$ sidebands (low-mass 1.808–1.824 GeV/c^2 , high-mass 1.904–1.920 GeV/c^2). The peak at small d_0 is due to the prompt component. The broad distribution extending to large d_0 is due to the nonprompt component. The prompt and nonprompt components are each modeled with the sum of two Gaussians. The fraction f_B is determined in each time bin for the region $d_0 < 60 \mu\text{m}$, which is dominated by the prompt component. The time dependence of f_B is characterized by a five-parameter polynomial fit to the values from each time bin. The value of f_B is $(1.5 \pm 0.4)\%$ at $t/\tau = 1.4$ and increases with t/τ due to the faster decay rate of D^0 mesons compared to beauty particles. At $t/\tau = 6.4$, $f_B = (24 \pm 1)\%$. The function $R_B(t/\tau)$ can be

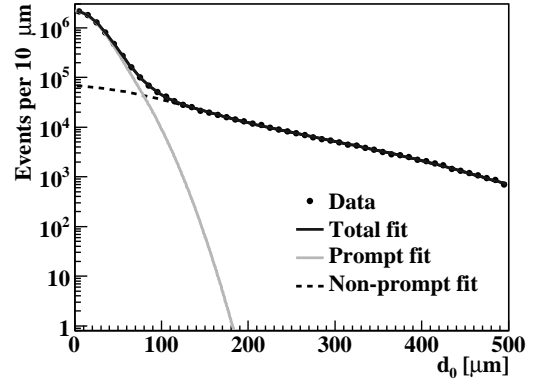


FIG. 3. Distribution of transverse impact parameter d_0 for right-sign D^0 candidates from all t/τ bins. The narrow peak is due to promptly-produced D^0 mesons and the broad distribution is due to nonprompt D^0 mesons from beauty-particle decay. For candidates with $d_0 < 60 \mu\text{m}$, 95% are produced promptly at the collision point and 5% are nonprompt.

expressed in terms of a function $H(t/\tau, t'/\tau)$ which gives the distribution of nonprompt D^0 decays versus t/τ for a given t'/τ , where t'/τ is measured from the decay point of the beauty particle. The function H is determined from a full detector simulation of beauty particle to D^* decays for the 20 bins of t/τ , and 100 bins of t'/τ . The

function $R_B(t/\tau)$ is given by

$$R_B(t_i/\tau) = \frac{\sum_{j=1}^{100} H(t_i/\tau, t'_j/\tau) R(t'_j/\tau)}{\sum_{j=1}^{100} H(t_i/\tau, t'_j/\tau)}, \quad (3)$$

where i and j denote the bins in t and t' . Note that R_B depends directly on the prompt D^* WS/RS ratio R defined in Eq. (1).

To fit for the mixing parameters, we define

$$\chi^2 = \sum_{i=1}^{20} \left[\frac{R_m(t_i/\tau) - R_m^{pred}(t_i/\tau)}{\sigma_i} \right]^2 + C_B + C_H, \quad (4)$$

where σ_i is the uncertainty on $R_m(t_i/\tau)$. The term C_B is a Gaussian constraint on the five fitted parameters describing $f_B(t/\tau)$, and C_H is a Gaussian constraint on the 2000 values of $H(t_i/\tau, t'_j/\tau)$. The statistical uncertainties on the $H(t_i/\tau, t'_j/\tau)$ are due to the number of events in the simulation. The mixing parameters R_D , y' , and x'^2 , and the Gaussian-constrained parameters for f_B and H are found by minimizing the χ^2 defined in Eq. (4).

To verify the self-consistency of the analysis procedure, we simulate distributions of $M_{K\pi}$ and ΔM for different assumed values of the mixing parameters R_D , y' , and x'^2 . We generate 400 samples for each of four different sets of mixing parameters. For each parameter set, the distributions of fitted parameters have mean values consistent with the input parameters.

We examine various sources of systematic uncertainty in the analysis procedure. The effect on the WS signal yields due to the uncertainty in the signal shapes used to fit the $M_{K\pi}$ and ΔM distributions is studied by independently varying the shape parameters by $\pm 1\sigma$. For each parameter, the resulting variation of the signal yield is negligible compared to the statistical uncertainty. We check the sensitivity of the WS and RS signals to the assumed shape of the $M_{K\pi}$ background by using simulations with alternative forms for the background shape. The alternative forms include explicit shapes for backgrounds due to $D^+ \rightarrow K^- \pi^+ \pi^+$ decays, determined from data, and partially reconstructed charm-particle decays, based on a full detector simulation. In both simulation studies, the mixing parameters are found to be consistent with those generated. To determine the sensitivity of R_m to R_B , we fit the d_0 distributions with an alternative shape function, leading to an alternate form for R_B with larger values at small t/τ . The resulting change in R_m is negligible, which can be understood from the small fraction of nonprompt D^* s at small t/τ . To check the sensitivity of R_m to $H(t/\tau, t'/\tau)$, we scale t/τ and t'/τ by $\pm 10\%$. The resulting changes in R_m are negligible compared to statistical uncertainties.

The results for the mixing parameters are given in Table I. The parameter values are highly correlated with correlation coefficients of -0.97 for the (R_D, y') term, 0.90 for (R_D, x'^2) , and -0.98 for (y', x'^2) . The resulting

functions $R_m^{pred}(t/\tau)$ and $R(t/\tau)$, describing the prompt component, are shown in Fig. 2. The two functions differ at large t/τ due to the effect of nonprompt D^* production. As shown in Table I, our results for the mixing parameters are consistent with previous measurements and our measurement of x'^2 is comparable in precision to that from LHCb.

TABLE I. Mixing parameter results and comparison with previous measurements. All results use $D^0 \rightarrow K^+ \pi^-$ decays and fits assuming no CP violation. The uncertainties include statistical and systematic components. The significance for excluding the no-mixing hypothesis is given in terms of the equivalent number of Gaussian standard deviations σ .

Expt.	$R_D (10^{-3})$	$y' (10^{-3})$	$x'^2 (10^{-3})$	$\sigma(\text{no mix.})$
This meas.	3.51 ± 0.35	4.3 ± 4.3	0.08 ± 0.18	6.1
Belle [17]	3.64 ± 0.17	$0.6^{+4.0}_{-3.9}$	$0.18^{+0.21}_{-0.23}$	2.0
BABAR [3]	3.03 ± 0.19	9.7 ± 5.4	-0.22 ± 0.37	3.9
CDF [5]	3.04 ± 0.55	8.5 ± 7.6	-0.12 ± 0.35	3.8
LHCb [7]	3.52 ± 0.15	7.2 ± 2.4	-0.09 ± 0.13	9.1

A fit assuming no mixing, shown in Fig. 2, is clearly incompatible with the data. We quantify this incompatibility using both Bayesian and frequentist methods. We define a likelihood $\mathcal{L} = \exp(-\chi^2/2)$, normalized over the mixing parameter space, with χ^2 as defined in Eq. (4). We compute contours bounding a region with a given value of Bayesian posterior probability. A uniform prior is used for R_D , y' , and x'^2 , and R_D is treated as a nuisance parameter. The contours are shown in Fig. 4. The no-mixing point, $y' = x'^2 = 0$, lies on the contour corresponding to 6.1 Gaussian standard deviations. If the physical restriction $x'^2 > 0$ is imposed, there is no change in the no-mixing significance. Using alternative priors, uniform in x' or y'^2 , the no-mixing significance is 6.3 σ . A frequentist test statistic $\Delta\chi^2$ is formed from the difference in χ^2 between a fit with $y' = x'^2 = 0$ and a fit with all three mixing parameters floating. For the data, $\Delta\chi^2 = 58.75 - 16.91 = 41.84$. A frequentist p -value is obtained by simulating mass distributions for $y' = x'^2 = 0$ and evaluating $\Delta\chi^2$ using the same procedure as for data. In 10^{10} samples, 6 are found with $\Delta\chi^2 > 41.8$, giving a p -value corresponding to 6.1 σ .

In summary, we measure the time dependence of the ratio of decay rates for $D^0 \rightarrow K^+ \pi^-$ to the Cabibbo-favored decay $D^0 \rightarrow K^- \pi^+$. A signal of 3.3×10^4 $D^{*+} \rightarrow \pi^+ D^0$, $D^0 \rightarrow K^+ \pi^-$ decays is obtained with proper decay times between 0.75 and 10 mean D^0 lifetimes. The data sample recorded with the CDF II detector at the Fermilab Tevatron corresponds to an integrated luminosity of 9.6 fb^{-1} for $p\bar{p}$ collisions at $\sqrt{s} = 1.96 \text{ TeV}$. Assuming CP conservation, we measure the D^0 - \bar{D}^0 mixing parameters to be $R_D = (3.51 \pm 0.35) \times 10^{-3}$, $y' = (4.3 \pm 4.3) \times 10^{-3}$, and $x'^2 = (0.08 \pm 0.18) \times 10^{-3}$,

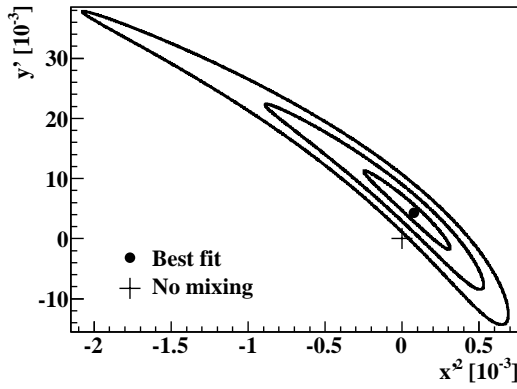


FIG. 4. Contours in $x'^2 - y'$ parameter space bounding regions with Bayesian posterior probability corresponding to 1, 3, and 5 Gaussian standard deviations.

providing important accuracy for the world averages. We report contours in the $x'^2 - y'$ plane which bound regions of a given Bayesian posterior probability; we find that the significance of excluding the no-mixing hypothesis is equivalent to 6.1 Gaussian standard deviations, thus confirming the observation of $D^0 - \bar{D}^0$ mixing.

We thank the Fermilab staff and the technical staffs of the participating institutions for their vital contributions. This work was supported by the U.S. Department of Energy and National Science Foundation; the Italian Istituto Nazionale di Fisica Nucleare; the Ministry of Education, Culture, Sports, Science and Technology of Japan; the Natural Sciences and Engineering Research Council of Canada; the National Science Council of the Republic of China; the Swiss National Science Foundation; the A.P. Sloan Foundation; the Bundesministerium für Bildung und Forschung, Germany; the Korean World Class University Program, the National Research Foundation of Korea; the Science and Technology Facilities Council and the Royal Society, UK; the Russian Foundation for Basic Research; the Ministerio de Ciencia e Innovación, and Programa Consolider-Ingenio 2010, Spain; the Slovak R&D Agency; the Academy of Finland; the Australian Research Council (ARC); and the EU community Marie Curie Fellowship contract 302103.

* Deceased

† With visitors from ^aUniversity of British Columbia, Vancouver, BC V6T 1Z1, Canada, ^bIstituto Nazionale di Fisica Nucleare, Sezione di Cagliari, 09042 Monserrato (Cagliari), Italy, ^cUniversity of California Irvine, Irvine, CA 92697, USA, ^dInstitute of Physics, Academy of Sciences of the Czech Republic, 182 21, Czech Republic, ^eCERN, CH-1211 Geneva, Switzerland, ^fCornell University, Ithaca, NY 14853, USA, ^gUniversity of Cyprus,

Nicosia CY-1678, Cyprus, ^hOffice of Science, U.S. Department of Energy, Washington, DC 20585, USA, ⁱUniversity College Dublin, Dublin 4, Ireland, ^jETH, 8092 Zürich, Switzerland, ^kUniversity of Fukui, Fukui City, Fukui Prefecture, Japan 910-0017, ^lUniversidad Iberoamericana, Lomas de Santa Fe, México, C.P. 01219, Distrito Federal, ^mUniversity of Iowa, Iowa City, IA 52242, USA, ⁿKinki University, Higashi-Osaka City, Japan 577-8502, ^oKansas State University, Manhattan, KS 66506, USA, ^pBrookhaven National Laboratory, Upton, NY 11973, USA, ^qUniversity of Manchester, Manchester M13 9PL, United Kingdom, ^rQueen Mary, University of London, London, E1 4NS, United Kingdom, ^sUniversity of Melbourne, Victoria 3010, Australia, ^tMuons, Inc., Batavia, IL 60510, USA, ^uNagasaki Institute of Applied Science, Nagasaki 851-0193, Japan, ^vNational Research Nuclear University, Moscow 115409, Russia, ^wNorthwestern University, Evanston, IL 60208, USA, ^xUniversity of Notre Dame, Notre Dame, IN 46556, USA, ^yUniversidad de Oviedo, E-33007 Oviedo, Spain, ^zCNRS-IN2P3, Paris, F-75205 France, ^{aa}Universidad Tecnica Federico Santa Maria, 110v Valparaiso, Chile, ^{bb}The University of Jordan, Amman 11942, Jordan, ^{cc}Universite catholique de Louvain, 1348 Louvain-La-Neuve, Belgium, ^{dd}University of Zürich, 8006 Zürich, Switzerland, ^{ee}Massachusetts General Hospital, Boston, MA 02114 USA, ^{ff}Harvard Medical School, Boston, MA 02114 USA, ^{gg}Hampton University, Hampton, VA 23668, USA, ^{hh}Los Alamos National Laboratory, Los Alamos, NM 87544, USA, ⁱⁱUniversità degli Studi di Napoli Federico I, I-80138 Napoli, Italy

- [1] J. Beringer *et al.* (Particle Data Group), Phys. Rev. D **86**, 010001 (2012).
- [2] D. Asner, Review article on $D^0 - \bar{D}^0$ mixing in [1], pp. 903–909.
- [3] B. Aubert *et al.* (BABAR Collaboration), Phys. Rev. Lett. **98**, 211802 (2007).
- [4] M. Staric *et al.* (Belle Collaboration), Phys. Rev. Lett. **98**, 211803 (2007).
- [5] T. Aaltonen *et al.* (CDF Collaboration), Phys. Rev. Lett. **100**, 121802 (2008).
- [6] J. Lees *et al.* (BABAR Collaboration), Phys. Rev. D **87**, 012004 (2013).
- [7] R. Aaij *et al.* (LHCb Collaboration), Phys. Rev. Lett. **110**, 101802 (2013).
- [8] S. Bianco, F. Fabbri, D. Benson, and I. Bigi, Riv. Nuovo Cim. **26N7**, 1 (2003).
- [9] A. F. Falk, Y. Grossman, Z. Ligeti, Y. Nir, and A. A. Petrov, Phys. Rev. D **69**, 114021 (2004).
- [10] M. Ciuchini, E. Franco, D. Guadagnoli, V. Lubicz, M. Pierini, V. Porretti, and L. Silvestrini, Phys. Lett. B **655**, 162 (2007).
- [11] E. Golowich, J. Hewett, S. Pakvasa, and A. A. Petrov, Phys. Rev. D **76**, 095009 (2007).
- [12] G. Blaylock, A. Seiden, and Y. Nir, Phys. Lett. B **355**, 555 (1995).
- [13] R. Godang *et al.* (CLEO Collaboration), Phys. Rev. Lett. **84**, 5038 (2000).
- [14] D. Acosta *et al.* (CDF Collaboration), Phys. Rev. D **71**, 032001 (2005).
- [15] A. Abulencia *et al.* (CDF Collaboration), Phys. Rev. D **74**, 031109 (2006).
- [16] T. Aaltonen *et al.* (CDF Collaboration), Phys. Rev. D **85**, 012009 (2012).

- [17] L. Zhang *et al.* (Belle Collaboration), Phys. Rev. Lett. **96**, 151801 (2006).